Quantum Critical Heavy Fermion Metal $YbRh_2Si_2$

Gertrud Zwicknagl

Institut für Mathematische Physik, Technische Universität Braunschweig, Mendelssohnstr. 3, 38106 Braunschweig,Germany

The evolution with magnetic fields of the heavy f-derived quasiparticles in $YbRh_2Si_2$ and the temperature dependence of the 4f spectral function in ambient field are calcualted by means of the Renormalized Band method. The Zeeman splitting of the Kondo resonance induces a series of Lifshitz transitions. The theoretically predicted critical magnetic fields agree quantitatively with the positions of anomalies in transport properties. To calculate the 4f spectral function of the periodic solid we use the single-impurity many-body t-matrix for the f-channels. We find that the dispersive heavy quasiparticle structures persist up to rather high temperatures in agreement with recent ARPES experiments. Implications for the interpretation of the observed "anomaly line" are discussed.

1. Introduction

Understanding the collective electronic properties of emergent materials remains a great challenge to condensed-matter theory[1]. Important examples are transition metal oxides, metals containing lanthanide or actinide atoms and organic conductors. At low temperatures, these materials exhibit novel phenomena like metal-to-insulator transitions, heavy fermions, unconventional superconductivity and unusual magnetism. The quantum mechanical ground states are determined by subtle compromises between varoius interactions. The resulting high sensitivity with respect to external fields will allow for new functionalities and novel technical applications.

Figure 1 schematically displays the generic phase diagram common to many materials with strongly correlated electrons. Depending on temperature T and some external control parameter - here denoted by g - phases with long-range "conventional" order or normal paramagnetic Fermi liquids and Quantum Phase Transitions (QPTs), i. e., changes in the quantum mechanical ground state at $T = 0K$ are encountered[2]. It is rather common that the Quantum Critical Point (QCP) at g_c lies beneath a "superconducting dome".

A QPT cannot be directly observed since it occurs at $T = 0$ by definition. The quantum fluctuations associated with a QCP, however, affect the thermodynamic and transport properties at finite temperatures giving rise to the anomalous behavior of the "strange metal" [3–6].

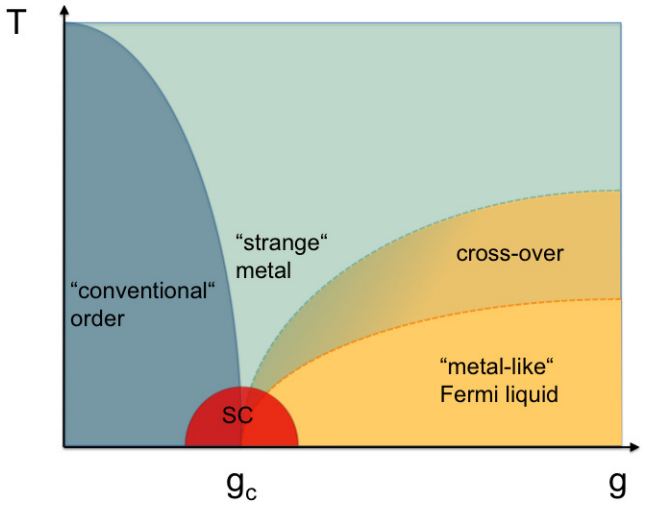

Fig. 1. Generic phase diagram of materials with strongly correlated electrons From left to right: Schematic phase diagram denoting the various low-temperature phases.

The important question is whether one can define universality classes for QPTs in close analogy to the well-studied thermal phase transitions. An undispensible pre-requisite for an answer is to know how the phases evolve when the system is tuned through the QCP. This, in turn, requires a detailed microscopic characterization of the ground states involved.

The focus of the present article are the low-temperature phases of heavy-fermion materials. The latter are usually inter-metallic compounds with lanthanide or actinide ions on regular lattice sites. Of particular interest in the context of QPTs are Ce- or Yb-systems which can be tuned continuously from a magnetically ordered to a non-magnetic ground state. The anomalous behavior in the vicinity of the QPC results from the degrees of freedom of the partially filled 4f shells.

The non-magnetic state is a Fermi liquid which results from a Kondo effect [7]. The strongly renormalized "heavy" quasiparticles can be viewed as composites involving the magnetic 4f degrees of freedom and the conduction

electrons. The magnetically ordered phases, on the other hand, can be described in terms of conduction electrons which weakly interact with local 4f moments.

How does the magnetic order appear when the system is tuned from the Fermi liquid through the QCP? Two different scenarios are discussed for the QCPs in heavy-fermion materials: First, the heavy quasiparticles can form a Spin Density Wave (SDW) due to the residual interaction. This "conventional" QCP is found in various stochiometric Ce-systems like e. g. $CeCu_2Si_2$. The second more radical scenario assumes that the heavy quasiparticles disintegrate into their constituents at the critical value g_c. The existence of such an "unconventional QCP" is the working hypothesis for $YbRh_2Si_2$ where the magnetic field is a convenient tuning parameter. As a consequence, the anomalies along the "anomaly line" at elevated temperatures and finite magnetic fields are attributed to the disintegration of the heavy quasiparticles.

To assess the validity of this assumption it is important to identify the states in $YbRh_2Si_2$ which are separated by the QCP. The properties of a metal with conventional magnetic order of local moment can be successfully and quantitatively described by usual ab initio electronic structure methods. These schemes, however, fail for the renormalized Fermi liquid state.

We adopt the Renormalized Band (RB) method which successfully describes the heavy quasiparticles in Ce-based heavy fermions. The ansatz is extended to calculate the 4f spectral function at elevated temperatures.

The paper is organized as follows: After a brief overview in Section 2, we summarize the characteristic properties of heavy-fermion systems in Section 3. In Section 4, we demonstrate for an exactly soluble model that the approximations underlying traditional ab initio band structure calculations fail to capture the characteristic features of the low-energy excitations in heavy-fermion systems. The Renormalized Band method is introduced in Section 5 and applied to $CeRu_2Si_2$ and $CeCu_2Si_2$ in Section 6. In Section 7, we present the RB results for $YbRh_2Si_2$. The influence of an external magnetic field is investigated in Section 8 and the variation with temperature of the $4f$ spectral function is considered in Section 9. The paper closes with a summary and an outlook in Section 10

2. Many-electron systems

The electronic structure problem for a solid is one of many interacting fermions (electrons) moving in a lattice. The properties of these systems are generally determined by the interplay of two types of influences. First, there is a tendency towards delocalization which is a consequence of the fact that wave functions at neighboring lattice sites overlap. It favors the formation of a conventional band spectrum and one-electron Bloch states in which the itinerant electrons are distributed throughout the entire crystal. Second, the electrons interact via the repulsive Coulomb interaction which leads to localization and the probability for hopping from one site to another will depend on whether the final site is occupied or empty. A strong Coulomb interaction between two electrons at the same lattice site would favor the formation of local magnetic moments which can be observed in the magnetic susceptibility. The general theoretical problem has proved too difficult for an exact analysis. Approximate solutions can be found only in limiting cases.

The traditional electron theory of metals which is based on the Sommerfeld-Bethe model[8] emphasizes the aspect of delocalization. Starting from the picture of free electrons the model sucessfully explains the existence of Fermi surfaces and a wide range of thermodynamic properties. Typical examples are the electronic contribution to the specific heat at low temperatures which varies linearly with temperature $C \simeq \gamma T \ldots$ with a proportionality factor of order $\gamma \simeq 1 mJ/MoleK^2$ as well as the magnetic susceptibility which approaches a temperature-independent value reflecting the non-magnetic character of the ground state.

The "free" electron picture was justified by Landau in his famous theory of Fermi liquids[9–12] which provides a highly useful conceptual framework for describing interacting Fermi systems. The fundamental conceptual basis is the notion of "adiabatic continuity" which should prevail if the interaction is gradually turned on [5]. As states of similar symmetry do not cross during this adiabatic process there should result a one-to-one correspondence between the well-known free fermion states and their unknown complex counterparts in the interacting system. In particular, the character of the ground states are the same, i. e., filled Fermi seas. The low-energy excitations can be described to good approximation in terms of a single-particle spectrum. This important fact is a direct consequence of the Pauli principle. The single-particle excitations or "quasi-particles" are characterized by momentum and spin and obey Fermi statistics. They can be visualized as

composite objects consisting of the bare particle (electron) and some kind of polarization cloud which results from the Coulomb correlations. The many-body effects modify the energy dispersion relation and the interactions of the quasi-particles. The one-to-one correspondence implies in general that the interactions do not change the volume enclosed by the Fermi surface. This statement is commonly referred to as Luttinger's theorem[13,14]. Today, Landau's Fermi liquid theory is the "standard model" for the modern electron theory of metals.

The most difficult aspect of the quasiparticle description is the evaluation of the Coulomb correlation effects. Landau's semiphenomenological approach uses experimental data to replace direct calculations of these effects.

Density Functional Theory (DFT) introduced by Hohenberg, Kohn and Sham[15,16]provides an efficient and rather accurate method to explicitly construct effective potentials required for material specific calculations. The fundamental quantity of the theory is the (inhomogeneous) electron density in the ground state which is to be determined selfconsistently. The theory allows for parameter-free calculations of the ground state properties[17]. The method yields ficticious energy eigenvalues which are usually very good approximations to the physical energy levels in conventional metals. For reviews see[18–21]. Combined with highly efficient numerical methods for solving the Schrdinger equation this ab-initio method greatly helped to understand ordinary metals and their (ground state) properties.

The break-down of the Landau Fermi liquid theory at the transition from the normal into the superfluid or superconducting state can be described by introducing the concept of broken symmetry[22]. According to this ansatz, phase transitions occur via symmetry reduction which is described in terms of an order parameter. The latter characterizes the appearance of long- range correlations - the pair-correlations in superconductors. Similar examples are the formation of a Charge Density Wave (CDW) or a Spin Density Wave (SDW). The framework described above consistently and successfuly describes the behavior of "ordinary" metals. In the spirit of Landau, the starting point is the picture of non-interacting electrons moving in effective potentials which also account for electron-electron interaction effects. The DFT provides a highly sophisticated scheme for explicitly constructing the effective potentials. The electron states provide the basis for understanding the collective dynamics which affects the response to external perturbations and phase transitions where long-range correlations are accounted for by symmetry-breaking.

In emergent materials, the correlation effects, i. e., the deviations from the anticipated behavior of independent electrons result from partially filled inner d- or f-shells. From a theorist's point of view, these materials lie at the intersection of a large number of long--standing problems in the physics of metals. We immediately face the fundamental question which picture provides the better starting point for theoretical models, a delocalized description in terms of energy bands or a localized representation which properly accounts for the atomic properties.

The general problem manifests itself in the transition metals whose d-electrons exhibit both aspects. This fact was the origin for the historical controversy between Slater [23] emphasizing the band picture and VanVleck [24] who advovated a description of the d-electrons in terms of local magnetic moments. The latter model explains various features found at elevated temperatures (or energies). Examples are the Curie-Weiss susceptibility observed in ferromagnetic transition metals above the ordering temperature. On the other hand, typical low-temperature properties such as the relatively large Sommerfeld coefficient could only be understood when the d-electrons were treated as itinerant band states. The band picture is also consistent with the non-integral Bohr magneton number per atom of the observed spontaneous magnetization. Direct evidence for the delocalized character of the d-electrons, as far as the low-energy excitations are concerned, is the fact that they contribute to the Fermi surface (see e. g. [25]). To summarize, the answer to the question which of the above-mentioned pictures is the appropriate starting point seems to depend on the physical quantities under consideration. This is a consequence of the electronic correlations. There is no doubt that the d-electrons are delocalized despite the fact that some atomic features persist. The correlations restrict the energy or temperature range where the Fermi liquid picture is valid.

Having in mind the scenario encountered for the d-electrons we next turn to the case of the f-electrons. The corresponding wave functions are much more localized than the highest occupied atomic d-levels. The intra-atomic Coulomb repulsion is much larger than the estimated band widths which seems to favor a localized picture. It was shown, however, that the f-electrons should also be described in within a band picture as delocalized states as far as the low-energy excitations in heavy fermion compounds are concerned.

3. Heavy fermions in 4f systems

Heavy fermion systems are primarily intermetallic compounds in which one of the constituents is a rare earth or actinide ion with a partially filled f-shell. Some of the best known examples are Ce- and Yb-based compounds as well as the U- and Pu-based systems. The f-states are well localized, i. e., the corresponding charges are more or less confined within spheres with the ionic radii. As a consequence, the f-states are expected to preserve their atomic character. The strong Coulomb interactions among the 4f- electrons at each atomic site can lead to a variety of magnetic effects.

The key features which are responsible for the unusual behavior of heavy fermion compounds are the degeneracy which is associated with the partially filled f-shells and the weak hybridization with the delocalized conduction states. Their interplay leads to anomalies in the variation with temperature of many experimental properties (for recent reviews see[26–28]).

As a consequence of the strong correlations, it is not possible to describe the influence of the f-states in terms of a unique simple model[29,30]. Instead, new energy scales appear. In the high-temperature regime for $T \gg T^*$ with $k_B T^*$ of the order of $1meV$, the degrees of freedom associated with the partially filled f-shells are conveniently modelled by local magnetic moments which weakly interact with the conduction electrons. The variation with temperature of the specific heat exhibits pronounced Schottky anomalies corresponding to crystalline effective field (CEF) excitations while the magnetic susceptibility is Curie-Weiss-like reflecting the magnetic moment of the partially filled f-shell. These findings suggest that the f-electrons can be considered as part of the ion cores in viewing the band structures of heavy fermion compounds. The number of quasiparticles which determines the volume enclosed by the Fermi surface is given by the number of conduction electrons and, concomitantly, equals the nominal chemical valence. The Fermi surface is "small". The coupling between the conduction electrons and the f-states becomes strongly evident as the temperature is lowered. For $T \simeq T^*$, the resistivity rises like in magnetic alloys indicating some kind of Kondo effect in lanthanide heavy fermion systems, i. e., the local spin-degrees of freedom at the f-sites are strongly coupled to the conduction electrons forming (local) singlets with them. The Kondo picture has been confirmed by the observation of the Kondo resonance which forms at low temperatures[31,32].

At low temperatures coherence is built up between the f-sites and the resistivity approximately follows $\rho(T) = \rho_0 + AT^2$ as predicted by Fermi

liquid theory. The specific heat varies approximately linearly with temperature (that is, $C = \gamma T + \dots$), and the magnetic susceptibilty, χ_s, approaches a Pauli-like form, becoming almost independent of temperature. The values of the coefficients γ are of the order of $J/MolK^2$ and consequently several order of magnitude larger than those of ordinary metals which are of the order of $\simeq mJ/MolK^2$. Due to the large Sommerfeld coefficient of the electronic specific heat which can be written in terms of an effective mass m^* of the quasiparticles these materials have been termed heavy fermion compounds. The magnetic susceptibility χ_s is enhanced by a factor of comparable magnitude. These findings suggest that heavy fermion compounds form a coherent Fermi liquids at sufficiently low temperatures. Many well-known relations derived for independent electrons are satisfied provided the huge effective mass of the quasiparticles is properly accounted for. This is achieved by replacing the Fermi energy E_F which is typically of order 10 eV in a conventional metal by the characteristic energy $k_B T^*$ which is of order 1meV.

While these findings unambiguously show that the low-energy excitations are heavy quasiparticles involving the f degrees of freedom, they nevertheless do not provide conclusive information on how the latter have to be incorporated into a Fermi liquid description. A characteristic property of a Fermi liquid is the existence of a Fermi surface whose volume is determined by the number of itinerant fermions. It is rather obvious that at high temperatures the f electrons should be excluded from the Fermi surface due their apparent localized character. The latter, however, is lost at low temperatures. The conjecture that the f-degrees of freedom have to be treated as itinerant fermions and, consequently, have to be included in the Fermi surface was met with great scepticism[33]. This hypothesis implies that the strong local correlations in Kondo lattices lead to an observable many-body effect, i. e., the change with temperature of the volume of the Fermi surface. This unusual behavior[30] was confirmed experimentally by measurements of the de Haas-van Alphen (dHvA) effect[34–36] and recent photoemission studies[37,38].

There is a competition between the formation of (local) Kondo singlets and the lifting of degeneracies by long-range magnetic order. In the high-temperature regime the moments of the Ce 4f- shells are coupled by the RKKY interaction which can favor parallel as well as antiparallel orientation of the moments at neighboring sites. Model calculations for two Kondo impurities[39–41] showed that antiferromagnetic correlations between the magnetic sites weaken the Kondo singlet formation reducing the char-

acteristic energy scale kT* to rather small values. Consequences for an extended lattice will be discussed in the subsequent section on Quantum Phase Transitions.

4. Kondo effect: Molecular model

In this section we show that the low-energy physics of a Kondo system cannot be captured by traditional methods of electronic structure calculation like the Self Consistent Field (SCF) or Hartree-Fock approximation (HF) and the Density Functional Theory (DFT). This is demonstrated for a simple model which can be solved in closed form. Comparing the exact results to the predictions of the approximation schemes allows to asses the validity of the above-mentioned popular schemes.

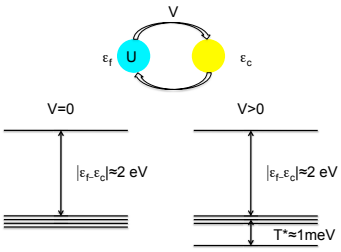

Fig. 2. Left panel: Simple Molecular Model and eigenvalues of the corresponding two-electron problem for $\epsilon_f < \epsilon_c \ll V$ in the limit of strong Coulomb repulsion $U \to \infty$. Due to the strong Coulomb repulsion among the f-electrons, the energetically most favorable two-electron states are obtained by occupying one f-state and one ligand state. This results in a fourfold degenerate ground state for vanishing hybridization. The spin degeneracy is lifted by hybridization with the doubly occupied ligand orbital. The low-energy singlet state is lowered relative to the triplet state by a small amount of energy $k_B T*$. Right panel: Schematic spectral function

Much of the essential physics of heavy fermion systems is already contained in the molecular model[42]

$$H = \epsilon_c \sum_\sigma c_\sigma^\dagger c_\sigma + \epsilon_f \sum_\sigma f_\sigma^\dagger f_\sigma + U \hat{n}_{f\uparrow} \hat{n}_{f\downarrow} + V \sum_\sigma \left(c_\sigma^\dagger f_\sigma + f_\sigma^\dagger c_\sigma \right) \quad (1)$$

where the weakly correlated conduction states of the metal are replaced by a two-fold degenerate extended ligand state such as an s-orbital. The corresponding creation (annihilation) operators will be denoted by $c_\sigma^\dagger$ (c_σ) where the index σ refers to the spin. The Coulomb repulsion in this extended orbital is rather weak and can be neglected. The strong correlations

are introduced by localized f-states which strongly repel one another. The corresponding creation, annihilation and number operators are denoted by $f_\sigma^\dagger$, f_σ and $\hat{n}_{f\sigma} = f_\sigma^\dagger f_\sigma$, respectively, where we consider only the spin degeneracy neglecting the orbital degrees of freedom. The actual value of the local Coulomb repulsion is of the order of $U \simeq 6eV$ in typical Ce compounds. These two subsystems are coupled through a weak hybridization V which is of the order of 0.1 eV in typical Ce systems. The orbital energies of the ligand state and the f-orbital are denoted by ϵ_c and ϵ_f, respectively, with $\epsilon_f < \epsilon_c$. In the following discussion, all energies will be measured relative to the orbital energy of the ligand state, ϵ_c. The hybridization V is rather small compared to the difference in the orbital energies i. e. $V \ll |\epsilon_f|$ whereas the Coulomb repulsion in the f-state is large i. e. $U \gg |\epsilon_f|$. This fact implies that many-particle states with two f-electrons are energetically unfavorable. For our qualitative considerations we shall assume $U \to \infty$ and consider only states where the f-orbital is empty (f^0-configuration) and where it is singly occupied (f^1-configuration). In addition, we shall focus on the two-electron states of the model Hamiltonian in Eq. (1). In the absence of hybridization (V=0), the ground state with $E = \epsilon_f$ is four-fold degenerate which is a direct consequence of the fact that the strong Coulomb repulsion among the f-electrons makes the f^2-configuration energetically unfavorable. The degeneracy is lifted by the hybridization between the ligand and the f-states. Since the latter conserves the spin it leaves the triplet states with $S = 1$ invariant but couples the two singlet states with $S = 0$. To leading order in the small ratio $x^2 = \frac{V^2}{|\epsilon_f|^2}$ the energy $\mathcal{E}$ of the singlet ground state is lowered by an amount $k_B T^* = \frac{2V^2}{|\epsilon_f|}$

$$\mathcal{E} = \epsilon_f - 2\,\frac{V^2}{|\epsilon_f|} + \ldots \tag{2}$$

The new energy scale $k_B T^*$ characterizes the low-energy excitations. The energy spectrum is schematically displayed in Figure 2.

The wave function of the ground state

$$|\psi_0\rangle \;=\; \left\{\sqrt{1-n_f}\,c_\uparrow^\dagger c_\downarrow^\dagger \;-\; \sqrt{n_f}\,\frac{1}{\sqrt{2}}\left(f_\uparrow^\dagger c_\downarrow^\dagger - f_\downarrow^\dagger c_\uparrow^\dagger\right)\right\}|0\rangle \tag{3}$$

has predominantly f^1-character but contains a small admixture of the f^0-configuration. The f-valence n_f is close to unity with

$$n_f \;=\; n_\uparrow \;+\; n_\downarrow \;=\; 1 - 2x^2 + \ldots \tag{4}$$

where $n_\uparrow, n_\downarrow$ are the occupancies of the two spin-degenerate f-states.

The molecular model qualitatively explains a number of properties which characterize dilute magnetic alloys and heavy fermion systems. For high temperatures $T \gg T^*$ the splitting separating the singlet ground state from the low-lying triplet excitations becomes irrelevant and the magnetic susceptibility hence reflects a magnetic moment. In the low-temperature regime $T \ll T^*$, on the other hand, the singlet character of the ground state becomes evident.

The dynamical magnetic susceptibility which can be measured by inelastic neutron scattering reflects the low-energy spin excitations with the excitation energy $\omega = k_B T^*$ corresponding to the singlet-triplet splitting. The molecular model also explains the qualitative variation with energy of the f-spectral function $\rho_f(\omega; T)$ which measures the probability of removing or adding an f-electron with energy ω and which can be directly measured by photoemission (PES) and inverse photoemission (BIS), respectively. The charge fluctuation peak corresponding to the $f^1 \to f^0$ transition is found for $\omega \simeq \epsilon_f$. The Abrikosov-Suhl (Kondo-) resonance $f^0 \to f^1$ at low energies $\omega \simeq k_B T^*$ is a direct consequence of the fact that the ground state contains a small admixture of the f^0 configuration which allows for adding an f-electron. The weight of this transition is given by $1 - n_f$ and hence is rather small. For increasing temperatures it melts away since triplet states with $n_f = 1$ become thermally populated. The high-energy part of the BIS spectrum with the $f^1 \to f^2$ transition is not contained in the present model which assumes $U \to \infty$.

The usual starting point for quantum chemical calculations is the Self Consistent Field or Hartree-Fock approximation where the two-electron interaction is replaced according to

$$U\hat{n}_{f\uparrow}\hat{n}_{f\downarrow} \to U < \hat{n}_{f\uparrow} > \hat{n}_{f\downarrow} + U\hat{n}_{f\uparrow} < \hat{n}_{f\downarrow} > -U < \hat{n}_{f\uparrow} >< \hat{n}_{f\downarrow} > \quad (5)$$

Here $< \hat{n}_{f\sigma} >= n_{f\sigma}$ denotes the expectation value of $\hat{n}_{f\sigma}$ in the ground state. The reduction in f-occupation as compared to the case of non-interacting electrons is simulated by the renormalization

$$\epsilon_{f\sigma} \to \epsilon_{f\sigma} + U < n_{f-\sigma} > \quad (6)$$

which raises the f-level above the ligand and hence suppresses double occupancies very effectively. The resulting effective single-particle states can be written as coherent superpositions of the (renormalized) f-states and the ligand orbitals corresponding to bonding and anti-bonding combinations. The lowest Hartree Fock eigenvalue E_σ^{HF} yields the total groundstate en-

ergy (to leading order)

$$\mathcal{E}^{HF} = 2\,E_\sigma^{HF} - U\,n_{f\uparrow}\,n_{f\downarrow} = -\,3V\,\left(\frac{V}{U}\right)^{1/3} \tag{7}$$

The ground state energy of the two-electron system vanishes for $U \to \infty$ which reflects the fact that the electrons are predominantly in the ligand orbital. We should like to emphasize that the latter is almost orthogonal to the exact ground state since the overlap is close to zero. In addition, the excitation energies defined as the difference between occupied and unoccupied Hartree-Fock levels is of the order $(V^{\,2}\,U)^{1/3}$ whereas the energy difference between total Hartree-Fock energies for states with different f occupation is of the order U. Neither energy scale is correct.

To summarize, the SCF method cannot reproduce a non-magnetic (singlet) ground state with f-valence close to unity and low-energy excitations.

The Density Functional Theory is based on the Hohenberg-Kohn theorem[15]: For a given two-particle interaction and given kinetic energy operator the properties of a non-degenerate ground state such as the external potential V_{ext} and the ground state energy are determined by the ground state density. The ground state energy $\mathcal{E}\,[n]$ is a functional of the density $n(\mathbf{r})$ which is extremal for the exact ground state density. The external potential is eliminated by means of a Legendre transformation and the potential energy is explicitly split off. An important assumption which finally allows to perform calculations is that the exact ground state density distribution of the interacting systems can be represented by the density of a ficticious non-interacting system moving in an external (local) potential. The density distribution is hence evaluated in terms of effective single-electron orbitals which are chosen to be orthogonal. Finally, The kinetic energy of the interacting system is approximated by that of its non-interacting counterpart $\mathcal{F}^0\,[n]$ which is easily evaluated. This so-called non-interacting kinetic energy $\mathcal{F}^0$ and the Hartree term $\mathcal{E}_{Hartree}$ which both yield large contributions to the ground state energy are subtracted from the total energy density functional. The remaining exchange-correlation energy

$$\mathcal{E}_{xc} \;=\; \mathcal{F} - \mathcal{F}^0 - \mathcal{E}_{Hartree} \tag{8}$$

contains, in general, contributions both from the kinetic energy and the interaction term of the Hamiltonian. Stationarity of the total energy requires the single-electron orbitals to satisfy the Kohn-Sham-equations[16]. The latter are effective Schrdinger equations where the (non-trivial) many-body effects in the ground state are contained in the exchange correlation

potential defined as

$$v_{xc} \;=\; \frac{\delta}{\delta n}\left[\mathcal{F}-\mathcal{F}^0-\mathcal{E}_{Hartree}\right] \tag{9}$$

Determining the many-particle ground state within DFT presupposes to find a reliable approximation for this static local potential v_{xc}. The molecular model can provide important insight into the DFT applied to strongly correlated electrons since the model can be solved in closed form. Therefore it is possible to determine the exact exchange-correlation energy $\mathcal{E}_{xc}$ as well as its derivative v_{xc} which fully account for the correlations in the ground state.

The static exchange-correlation potential v_{xc} containing - by construction - the correlations in the ground state is commonly used to calculate the low-energy excitations (quasiparticles) of an interacting electron system from the Kohn-Sham equations. The scheme which proved surprisingly successful for metals, however, does not correctly predict the small energy scale characterizing the f-derived low-energy excitations in heavy fermion materials.

The molecular model can be considered as a two-site problem as illustrated in Figure 2. The density distribution is characterized by the f-occupation n_f since the number of particles is fixed. The energy of the (effective) f-level $\tilde{\epsilon}_f$, on the other hand, plays the role of an external potential η while the hybridization is equivalent to a kinetic energy. An exact density functional is constructed in an straightforward way. According to the definition we subtract the potential contribution from the exact ground state energy Eq. (2) thereby expressing the f energy $\epsilon_f \equiv \eta$ in terms of the corresponding density distribution parameter $n \equiv n_f$ and the hybridization V. This procedure yields

$$\mathcal{F}\left[n\right] \;=\; -2\sqrt{2}V\sqrt{n}\sqrt{1-n} \qquad \text{for} \qquad U\to\infty \tag{10}$$

The large Coulomb interaction $U \to \infty$ does not permit the f valence to exceed unity. The expression for the density functional exhibits a remarkable symmetry with respect to the densities of the f electrons n and of the conduction electrons $1-n$. This fact can be interpreted as some kind of particle-hole symmetry in the 'lower Hubbard band' where double occupancies are strictly excluded.

Starting from the exact density functional we shall construct the exchange-correlation potential v_{xc} which accounts for the correlations in the ground state. The Hartree term which has to be subtracted is given by $\mathcal{E}_{Hartree} \;=\; \frac{1}{2}(n_\uparrow+n_\downarrow)\,U\,(n_\uparrow+n_\downarrow)$. According to the definition Eq. (9) we

also have to evaluate the kinetic energy for the non-interacting reference system. The latter is calculated from the eigenstates of two non-interacting particles in an external potential η with the density distribution characterized by

$$\mathcal{F}^0[n] = -2V\sqrt{n}\sqrt{2-n} \tag{11}$$

which exhibits conventional particle-hole symmetry as it is expected in the absence of interactions. For a detailled derivation we refer to[43].

Combining these results, the exchange-correlation potential as defined in Eq. (9) is seen to contain a contribution proportional to the Coulomb repulsion U. In strongly correlated systems, v_{xc} mainly acts so as to compensate the large Hartree term which leads to the wrong ground state in the SCF theory. The exchange-correlation potential cannot be considered as small in the limit $U \to \infty$. In addition, the separation of the interaction effects into Hartree and exchange-correlation potentials does not emerge as a natural concept in systems with strong *local* correlations.

Following Kohn-Sham, the excitation spectrum, i. e. the quasiparticle energies E_σ^{DFT}, are determined from the single-particle like Kohn-Sham equations. The effective potential at the f-site is a sum of the external potential, the Hartree contribution $v_{Hartree}$ and the exchange correlation potential v_{xc}. To illustrate the general structure of the excitation spectrum we do not have to explicitly evaluate the exchange-correlation functional. It is sufficient to know that the Kohn-Sham equations do exist. In the large U limit, we find

$$v_{xc}^{DFT} = -v_{Hartree} + \epsilon_f + 4x^2V + \dots \tag{12}$$

$$E_\sigma^{DFT} = -V + 2x^2V + \dots \tag{13}$$

The results for the large U limit are summarized as follows:

- The exchange correlation potential v_{xc} mainly compensates the Hartree term and does not describe the many-body aspects of the problem.
- The position of the f-level is renormalized by the effective potential. One obtains an effective f-level *above* the ligand state.
- The eigenvalues and hence the excitation energies scale with the *bare* hybridization V.

Since the ligand energy corresponds to the Fermi energy of a metal these results explain the failure of the standard band structure calculation in heavy fermion metals as shown qualitatively: the f-bands are shifted to the

Fermi energy but their bandwidth is much too broad. We should like to emphasize that this result is generally valid since the derivatation did not refer to an explicit expression for v_{xc} but only postulated its existence.

5. Renormalized Band Method

In the spirit of Landau, the Renormalized Band method introduces suitable parameters to construct a static not necessarily local potentials $V^{eff}(\mathbf{r}, \mathbf{r'})$ which accounts for the essential many-body aspects. These potentials are used to calculate the heavy quasiparticles by solving a band structure problem.

We would like to emphasize the predictive power of the Renormalized Band method as described below. Various unusual phenomena like the f-derived Fermi surface of $CeRu_2Si_2$, the SDW instability in $CeCu_2Si_2$ and the magnetic field induced Lifshitz transitions in $YbRh_2Si_2$ were first predicted theoretically and later confirmed experimentally - sometimes with a delay of up to several years. In the subsequent section, we shall give a brief summary of the method, the underlying ideas and the implementation. For a detailled description we refer to[29,44].

At this point we should like to add a technical remark. A number of different computational methods are available which solve band structure problems in a highly efficient way. The explicit form of the secular equation and, concomitantly, the choice of appropriate phenomenological parameters depend on the actual formulation of the problem as well as on the specific numerical procedure. Hence there are various different but equivalent schemes for introducing the renormalization.

The approach adopted here starts from a formulation of the band structure problem developed originally from scattering theory. The characteristic properties of a given material enter through the information about single center scattering which can be expressed in terms of properly chosen phase shifts $\{\eta_{\nu i}(E)\}$ specifying the change in phase of a wave incident on site i with energy E and symmetry ν with respect to the scattering center.

The central question encountered in this context is which quantities, in particular which phase shifts, reflect the many-body character of a specific system and, hence, have to be renormalized or, conversely, which phase shifts can be calculated directly from the ab-initio potentials generated within a standard electronic structure calculation. Microscopic models for the scattering off magnetic sites in dilute alloys serve as useful guidelines. In the case of rare-earth and actinide compounds, the T-matrix for the band

electron scattering is directly proportional to the Green's function of the localized states. As a consequence, we introduce renormalized phase shifts for waves which have the symmetry of the f-electron spin-orbit ground state multiplet, i. e., 4f j=5/2 for Ce systems with respect to the rare-earth or actinide sites.

Operationally, the renormalization procedure amounts to transforming the f-states of the spin-orbit ground state multiplet at the lanthanide site into the basis of CEF eigenstates $|m\rangle$ and introducing resonance-type phase shifts

$$\tilde{\eta}_{fm}(E) \simeq \arctan \frac{\tilde{\Delta}_f}{E - \tilde{\epsilon}_{fm}} \tag{14}$$

where the resonance width $\tilde{\Delta}_f$ accounts for the renormalized quasiparticle mass. The resonance energies $\tilde{\epsilon}_{fm} = \tilde{\epsilon}_f + \delta_m$ refer to the centers of gravity of the f-derived quasiparticle bands. Here $\tilde{\epsilon}_f$ denotes the position of the band center corresponding to the CEF ground state while the δ_m are the measured CEF excitation energies. One of the remaining two parameters, $\tilde{\epsilon}_f$, is determined by imposing the condition that the charge distribution is not altered significantly by introducing the renormalization. This makes the RB method a single-parameter scheme. As the 4f-count in Ce systems is slightly smaller than unity, $\tilde{\epsilon_f}$ will lie above the Fermi level. The free parameter, $\tilde{\Delta}_f$, is adjusted so as to reproduce the coefficient of the linear specific heat at low temperatures. The method has been shown to reproduce Fermi surfaces and anisotropies in the effective masses of a great variety of Ce-based compounds. In addition, it allows one to predict Fermi liquid instabilities. Typical results for Ce systems can be found in[26,27,45] and reference therein.

In calculating the coherent 4f-derived quasiparticle bands in the Yb-based heavy fermion compounds we essentially follow the procedure for the Ce-case as described above. We have to account for the fact that Yb can be considered as the hole analogue of Ce. Operationally this implies that we have to renormalize the 4f j=7/2 channels at the Yb sites instead of the 4f j=5/2 states in the Ce case. As the 4f hole count is slightly less than unity the center of gravity $\tilde{\epsilon}_f$ will lie below the Fermi energy. In addition, we have to reverse the hierarchy of the CEF scheme, i. e., $\tilde{\epsilon}_f < 0 \quad ; \quad \tilde{\epsilon}_{fm} = \tilde{\epsilon}_f - \delta_m \quad$. The parameters are schematically summarized in Figure 3

In the presence of a magnetic field, the quasiparticles have to be described by field-dependent parameters for the level $\tilde{\epsilon}_{fm}(h)$ and the reso-

nance width $\tilde{\Delta}_f(h)$. In the systems under consideration, the energy difference between the CEF ground state doublet and the excited states largely exceeds the resonance width. The latter is given by the characteristic energy $k_B T^*$ where T^* is of the order of the single-ion Kondo temperature. The low-temperature properties derived from the heavy quasiparticles will reflect the spatial symmetry of the CEF ground state wave function. The energy $h = \frac{1}{2} g_{eff} \mu_B H$ denotes the (anisotropic) Zeeman splitting of the free ion CEF ground state which is related to that of an effective spin-1/2-system by introducing anisotropic effective g-factors. In general, we anticipate the variation with magnetic field of the parameters $\tilde{\epsilon}_{fm}(h)$ and $\tilde{\Delta}_f(h)$ to be highly non-trivial due to the strong correlations.

The variation with magnetic field of the phase shifts in the low-field limit was discussed by Nozires[46] for dilute magnetic alloys. In his seminal paper he emphasized the importance of the molecular field correction . The latter accounts for the quasiparticle interactions which are reflected in the value $R = 2$ of the Sommerfeld-Wilson ratio. In our parametrization the molecular field correction translates into a correlation-enhanced Zeeman splitting of the centers of gravity $\tilde{\epsilon}_{fm}(h)$. The field-dependence of the renormalized band width $\tilde{\Delta}_f(h)$, however, cannot be derived from phenomenological considerations assuming "rigid" quasiparticles. In the present calculation, we use field-dependent parameters $\tilde{\epsilon}_f(h)$ and $\tilde{\Delta}_f(h)$ which are obtained from fits to field-dependent quasiparticle DOS of the single-impurity Anderson model[47–50]. The latter are calculated microscopically by means of the Numerical Renormalization Group (NRG) or, more conveniently, by Renormaized Perturbation Theory (RPT)[51–53]. This procedure properly accounts for the progressive de-renormalization of the quasiparticles with increasing magnetic field and the correlation-enhanced Zeeman splitting.

Having specified the parameters we next turn to a brief description of the actual implementation within the band structure scheme. The propagation from site i to site j of a state characterized by wave vector $\mathbf{k}$ is described by the structure constants $S^{ii'}_{\nu\nu'}(\mathbf{k})$. They specify the contribution of the wave outgoing from center i' with symmetry ν' to the incoming wave on center i with symmetry ν. The structure constants are usually evaluated in the angular momentum (ℓ, m)-basis; explicit expressions can be found e. g. in[54,55]. Since spin-orbit splitting is large compared to the width of the quasiparticle bands, a Dirac-relativistic formulation of the scattering problem in terms of the eigenfunctions of the total angular momentum $j = \ell + 1/2$ is more appropriate ((j, j_z)-representation). To account for CEF effects in heavy-fermion compounds we choose proper linear combinations

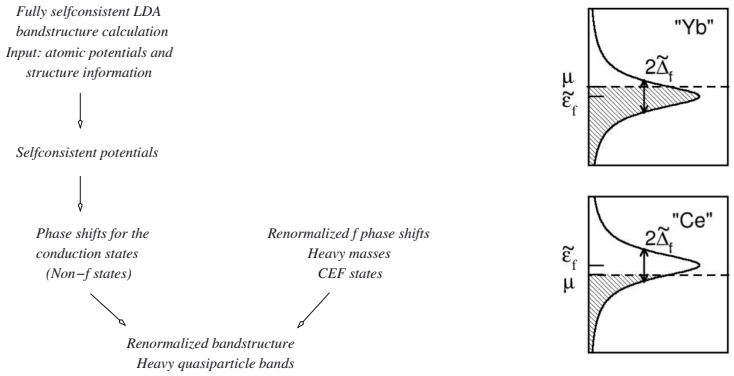

Fig. 3. Schematic summary of Renormalized Band calculation for metals with strongly correlated electrons (left panel). Comparison of typical quasiparticle DOS of Yb (upper right panel) and Ce (lower right panel) HFS. Since the number of 4f holes (Yb case) and electrons (Ce case) is slightly smaller than unity the corresponding band centers are below and above the Fermi energy, respectively

(Γ, γ_α) of the 4f$j = 5/2$ or 4f$j = 7/2$ states which are adapted to the local symmetry of the lattice site. The abbreviation ν may denote $\nu = (\ell, m)$, $\nu = (j, j_z)$ $\nu = (\Gamma, \gamma_\alpha)$, respectively. The quasiparticle energies $E_n(\mathbf{k})$ are solutions of the Linear Muffin Tin Orbita (LMTO) secular equation[54,55] in the Dirac-relativistic generalization[56]

$$\det\left(P^i_\nu(E)\,\delta_{\nu\nu'}\delta_{ii'} - S^{ii'}_{\nu\nu'}(\mathbf{k})\right) = 0 \tag{15}$$

where the potential functions $P^i_\nu(E)$ are closely related to the scattering phase shifts.

The secular equation Eq. (15) of the Renormalized Band scheme can be cast into the more familiar form of a hybridization model. For a detailled description of the general procedure and technical details we refer to the review[29]. The effective band Hamiltonian which reproduces the band structure in a narrow energy range surrounding the Fermi edge is a multi-band multi-orbital generalization of the model described by Hewson[7].

6. Heavy fermions in $CeRu_2Si_2$ and $CeCu_2Si_2$

To demonstrate the predictive power of the Renormalized Band method we discuss the Ce-based heavy fermion compounds $CeRu_2Si_2$ and $CeCu_2Si_2$

which crystallize in the tetragonal $ThCr_2Si_2$ structure with the unit cell displayed in Figure 4. The isostructural compounds CeM_2X_2 compounds in $ThCr_2Si_2$ structure where M = Cu, Ni, Ru, Rh, Pd, Au, .. and X = Si, Ge exhibit a great variety of ground states and have been extensively studied to clarify the interplay between the formation of magnetic order and heavy fermion behavior.

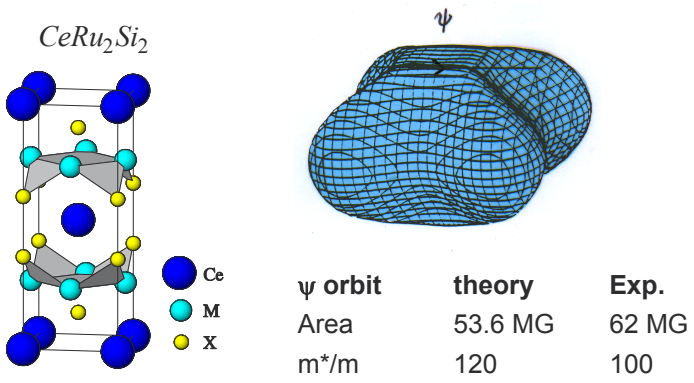

Fig. 4. $CeRu_2Si_2$: Conventional unit cell of the CeM_2X_2 compounds in $ThCr_2Si_2$ structure (left panel) and Fermi surface of the heavy quasiparticles (right panel).

The low-temperature behavior of $CeRu_2Si_2$ is well described by a paramagnetic Fermi liquid with weak residual interactions. The relevant low-energy excitations are heavy quasiparticles as inferred from the linear specific heat coefficient $\gamma \simeq 350$ mJ/molK^2 [57]. In the local moment regime, the Fermi surface is determined exclusively by the conduction states. The strongly renormalized Fermi liquid state, on the other hand, is described by the renormalized band method using $\tilde{\Delta}_f \simeq 10$ K in Eq. (14) for the intrinsic width of the quasiparticle band. The value is consistent with inelastic neutron data[58] as well as thermopower and specific heat data[57]. CEF effects are accounted for by adopting a Γ_7 ground state. The details of the calculation are described in Ref.[29].

The Renormalized Band scheme gives the correct Fermi surface topology for $CeRu_2Si_2$ and thus consistently explains the measured dH-vA data[29,30,59]. The measured quasiparticle masses are consistent with the coefficient of the linear specific heat[35,36,60]. This proofs that the heavy quasiparticles exhaust the low-energy excitations associated with the f-states.

The expected change in volume of the Fermi surface upon heating was

observed in recent photoemission experiments. Denlinger et al.[38] have shown that at temperatures around 25 K, the Fermi surface of $CeRu_2Si_2$, is that of its counterpart $LaRu_2Si_2$ which has no f electrons.

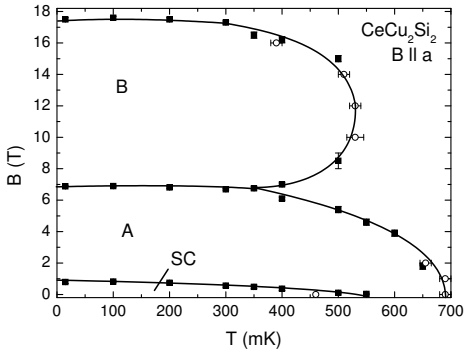

Fig. 5. B-T phase diagram of $CeCu_2Si_2$ for B ∥ a. Original version from Bruls et al.[61], completed version from Weickert et al.[62].

Let us now turn to the heavy fermion superconductor $CeCu_2Si_2$ which exhibits a highly complex phase diagram at low temperatures. This fact results from an extreme sensitivity of the physical properties with respect to variations of the stochiometry and external magnetic fields.

To calculate the quasiparticle bands in $CeCu_2Si_2$ by means of the Renormalized Band method, we adopt the CEF scheme suggested by[63]. The doublet ground state is separated from the excited states by an energy which is much larger than the characteristic energy of the heavy quasiparticles $T^* \simeq 10K$ (estimated from the γ-value).

The results for the Fermi surface[64,65] can be summarized as follows: We find two separate sheets of the Fermi surface for heavy and light quasiparticles. The light quasiparticles have effective masses of the order of $m^*/m \simeq 5$. They can be considered as weakly renormalized conduction electrons.

Of particular interest are heavy quasiparticles of effective masses $m^*/m \simeq 500$ which are found on a separate sheet which mainly consists of columns parallel to the tetragonal axis and of small pockets. The topology of the Fermi surface suggests that the strongly correlated Fermi liquid state should become unstable at sufficiently low temperatures. Firstly, it exhibits pronounced nesting features. Secondly, the topology of this surface

depends rather sensitively on the position of the Fermi energy. At low temperatures, a Lifshitz transition is found at a magnetic field of ∼7T where the transition into the B-phase is observed[64].

Much effort has been devoted to the characterization of the A phase whose the spin- density wave character was first inferred from resistivity results[66] and supported by specific heat and high-resolution magnetization measurements[67].

The important question in this context is: What is the origin of the antiferromagnetic correlations, how do they arise in the heavy fermion state and, finally how do they affect the heavy quasiparticles? The key to the answers comes from the Fermi surface of $CeCu_2Si_2$ and its nesting properties. As shown in Fig. 6 there are parallel portions which are connected by a wave vector close to $(1/4, 1/4, 1/2)$. As a consequence, the static susceptibility $\chi(\mathbf{q})$ exhibits a maximum for momentum transfer $\mathbf{q}$ close to the nesting vector (Fig . 6)

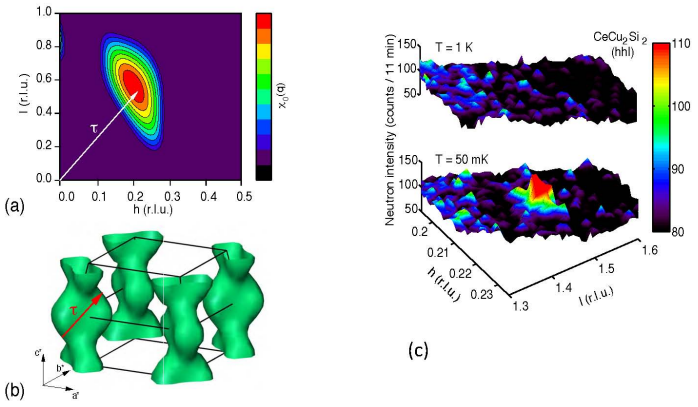

Fig. 6. $CeCu_2Si_2$: The static susceptibility $\chi(\mathbf{q})$ as calculated from the renormalized bands (a) exhibits a peak at the nesting vector $\boldsymbol{\tau}$ of the heavy Fermi surface (b). The experimental modulation vector appearing in the neutron diffraction intensity (c) below the A- phase transition temperature T_A shows perfect agreement with the calculated maximum position of $\chi(\mathbf{q})$.

Neutron scattering experiments[68] (Figure 6) for the stoichiometric compound (x=0) show a spin-density wave (SDW) which forms below $T_N \simeq 0.7$ K. The experimental propagation vector $\mathbf{Q}$ is close to (0.22,0.22,0.55) and the ordered moment amounts to $\mu \simeq 0.1\mu_B$. These findings show that the SDW in $CeCu_2Si_2$ arises out of the renormalized Fermi liquid state. The

transition is driven by the nesting properties of the heavy quasiparticles.

7. Heavy fermions in $YbRh_2Si_2$

$YbRh_2Si_2$ crystallizes in the tetragonal $ThCr_2Si_2$ structure. As the temperature vs. magnetic-field phase diagram exhibits numerous anomalies[69] this material has emerged as a prototypical system for investigation of quantum critical phenomena[70]. In its ground state, $YbRh_2Si_2$ orders antiferromagnetically below the Nel temperature, T_N=70 mK. By applying a weak magnetic field of B_c=60mT in the basal plane the magnetic order is suppressed[71] and the system is driven through a quantum critical point (QCP) into a strongly renormalized Landau Fermi Liquid (LFL) state. The changes of the ground state and the low-energy excitations across the QCP manifest themselves in numerous thermodynamic and transport properties. A prominent example is the Hall coefficient whose abrupt changes indicate Fermi surface reconstructions (see e. g.[70] and references therein).

The dispersion of the weakly-correlated non-f states is determined by a standard band structure calculation assuming the Yb ion is in $4f^{13}$ configuration. The effective potentials are generated selfconsistently within the Local Density Approximation (LDA) to Density Functional Theory (DFT). We refer to this calculation as f-core calculation. Details are given in[72]. The Fermi surface resembles that of the non-f reference compound $LuRh_2Si_2$[73].

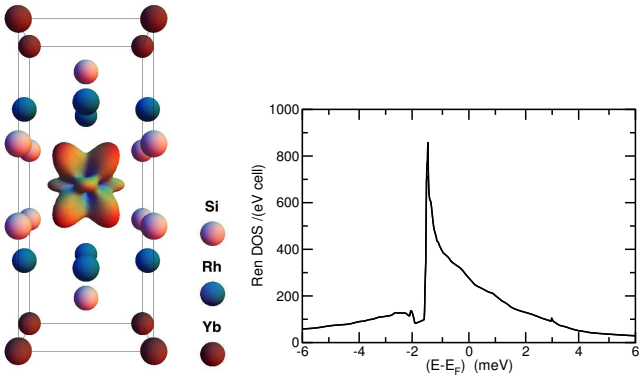

Fig. 7. $YbRh_2Si_2$: Left panel: Contour of equal 4f hole density for the CEF ground state of Yb^{+3}. The spheres denote the nearest heighbor atoms of the central Yb in the tetragonal body centered structure. Right panel: Zero-field quasiparticle DOS from RB calculation. The low-energy properties are determined by the peak at the Fermi energy. The expanded view shows a "coherence gap" and a van-Hove type singularity.

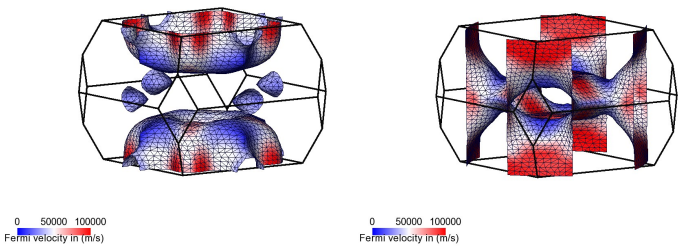

Fig. 8. $YbRh_2Si_2$: Major sheets of the quasiparticle Fermi surface (zero-field RB calculation). It consists of a Z-centered hole surface (left panel) and a multiply-connected surface ("jungle gym") (right panel. The modulus of the Fermi velocity is color-coded).

The RB scheme yields narrow bands with f-character in the vicinity of the Fermi energy while the dispersion of the broad non-f conduction bands remains essentially the same as in the local moment regime. The calculation assumed a Kondo temperature of $T_K = 25K$. The CEF energies and states were determined from the Inelastic Neutron Spectra (INS)[74,75] and the observed easy plane anisotropy in the magnetic susceptibility with g-factors are $g_{||}$=0.26 and $g_{\perp}$=3.79 for magnetic fields parallel to the tetragonal axis and in the basal plane. This yields the following values for the tetragonal CEF B_{20}=0.5246 meV, B_{40}=0.01195 meV, B_{60}=-0.0004725 meV, B_{44}=0.03598 meV, B_{64}=-0.01206 meV[44,76,77].

There are three bands intersecting the Fermi energy. In the following discussion, we shall neglect the small Γ-centered electron pocket and focus on the two bands giving rise to the two major sheets displayed in Figure 8. The overall topology qualitatively agrees with LDA results of Refs.[78–82]. The dominant contribution to the quasiparticle DOS and, concomitantly, to the specific heat and magnetic susceptibility comes from the Z-centered hole surface which has predominantly f-character. Following[83] we refer to this surface as "doughnut" although it is singly-connected, i. e., it has no hole). The states forming the "jungle gym", on the other hand, are strongly hybridized.

The quasiparticle DOS displayed in Figure 7 is mainly due to the ground state of the CEF-split 4f-states. The strongly anisotropic hybridization between the f-states and the conduction bands leads to pronounced van Hove-singularities in the DOS which correspond to changes in the topology of the iso-energy surfaces. These define four different energy regimes indicated by

vertical lines in the upper panel of Figure 9.

8. YbRh2Si2: Influence of magnetic field

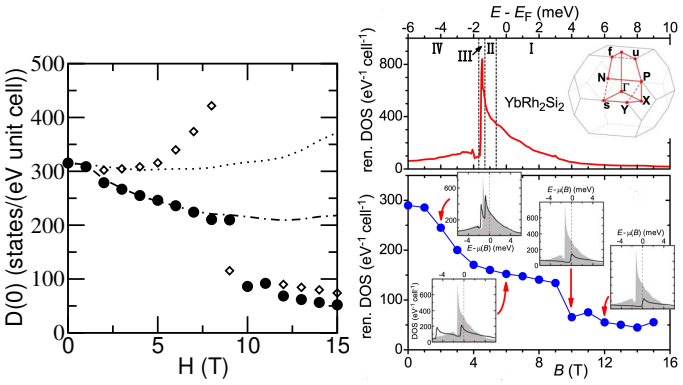

Fig. 9. $YbRh_2Si_2$: Left panel: Variation with magnetic field in the basal plane of the quasiparticle DOS at the Fermi level D(0) derived from the RB calculation (open circles). The field-dependent parameters $\tilde{\epsilon}_f(h)$ and $\tilde{\Delta}_f(h)$ are determined from fits to NRG calculations. Included for comparison are predictions assuming single-particle Zeeman splitting (dotted line), decreasing effective mass plus single-particle Zeeman splitting (dot-dashed line), correlation enhanced Zeeman splitting with zero-field effective mass (dashed line). The DOS deduced from the specific heat coefficient measured at ambient pressure[84] is shown for comparison (filled circles). Right panel: Quasiparticle DOS of YbRh2Si2 at B=0 as calculated from the Renormalized Band method (upper panel) and variation with magnetic field in the basal plane of the quasiparticle DOS at the Fermi energy (lower panel). The DOS at different magnetic fields displayed in the insets clearly show a Zeeman splitting of the van Hove singularity. The inset in the upper panel displays the Brillouin zone of the tetragonal body-centered lattice and the special points

The existence of these different regimes is reflected in the variation with magnetic field of the quasiparticle DOS at the Fermi energy. The characteristic features are (i) a continuous decrease resulting from the de-renormalization of the heavy quasiparticles and (ii) discontinuous changes at well defined values of the magnetic field resulting from Lifshitz transitions of the Fermi surface. The variation with magnetic field of the DOS at the Fermi energy agrees well with the measured DOS as can be seen from Figure 9.

The Lifshitz transitions in a magnetic field can be understood from simple qualitative considerations. The two major sheets, i. e., the doughnut and the jungle gym, can be described in terms of a hole surface centered at

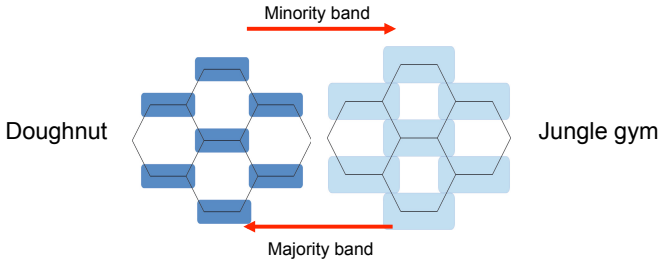

Fig. 10. Schematic illustration of the Lifshitz transitions between "doughnut" and "jungle gym" surfaces which are induced by variation of the hole number n_h.

the Z point (see Figure 8). The main distinguishing feature is the number of holes n_h. At ambient magnetic field, n_h is small for the doughnut and the Fermi surfaces in neighboring BZs are not connected. For the jungle gym, however, the Z-centered hole surfaces in different BZs are interconnected. In an external magnetic field, the number of holes increases in the minority bands while it decreases in their majority counterparts. At a critical value, the minority doughnut surface transforms into a jungle gym surface. In close analogy, the majority jungle gym surface will transform at some other critical field into a doughnut. This is schematically illustrated in Figure 10

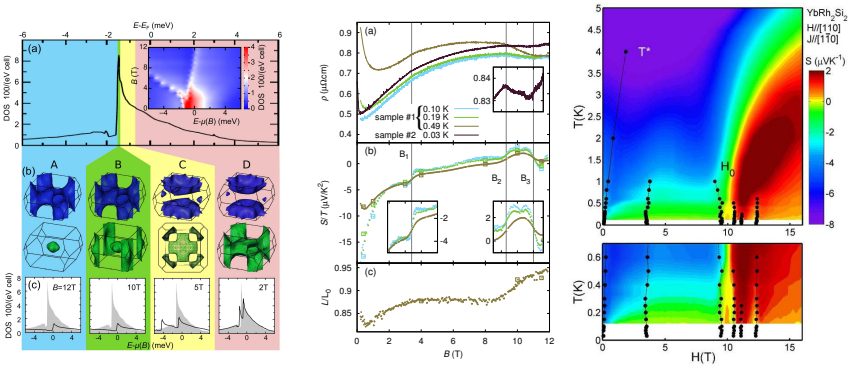

Fig. 11. Left panel: DOS at B=0T, Fermi surfaces and DOS at finite magnetic fields as calculated from the RB method. Middle and right panel: Field-induced anomalies in the transport properties from [85] (middle panel) and from [86] (right panel)

The series of Lifshitz transitions which occur at well-defined values of

the magnetic field are reflected in anomalies which have been found in the transport properties as shown in Figure 11.

A direct consequence of the field-induced Lifshitz transitions is that it is difficult to extract the shape of the Fermi surface from quantum oscillation experiments. These measurements are usually done in a field range where the Fermi surface topology differs from the one of the unperturbed system. In a field of ∼15T the "heavy" minority Fermi surface resulting from the doughnut should have a closed orbit in the 110 plane with area F=13kT and and effective mass m* ∼20m which agrees well with the values given by Westerkamp[87]. From Figure 12 it is obvious that the closed orbit is confined to a relatively narrow range of magnetic field orientations.

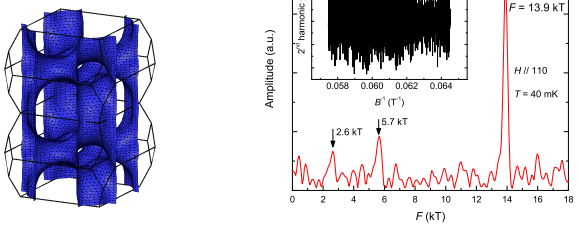

Fig. 12. $YbRh_2Si_2$: Multiply-connected sheet in high magnetic field of∼ 15T in the basal plane. There is a closed orbit with area ∼13kT and m* ∼ 20m in the 110 plane.

9. Finite temperatures: spectral function

The electronic band structure and the shape of the Fermi surface of $YbRh_2Si_2$ have been investigated by high-resolution Angle-Resolved Photoemission Spectroscopy (ARPES)[88]. The results displayed in Figure 13 clearly show that the Fermi surface is "large" in the absence of a magnetic field at $T = 10K$. This is concluded from the "open neck" at the $\bar{X}$-point. This characteristic feature of the "large" Fermi surface persists in a rather wide temperature range from $T = 1K$ up three to four times the Kondo temperature T_K as can be seen from Figure 14.

The observed behavior is reproduced by the calculated variation with temperature of the k-resolved f-spectral function $\rho(\mathbf{k};\omega)$. The latter is given in terms of the f-Green's function

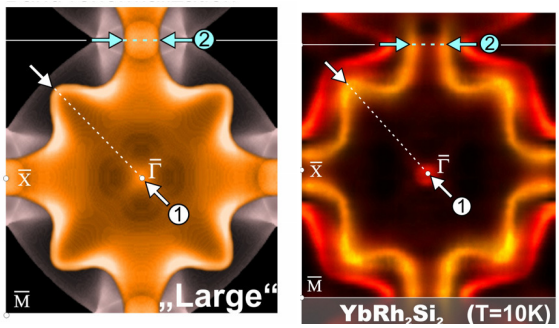

Fig. 13. $YbRh_2Si_2$: Left panel: Large Fermi surface from RB calculation. Right panel: Fermi surface from ARPES [88]

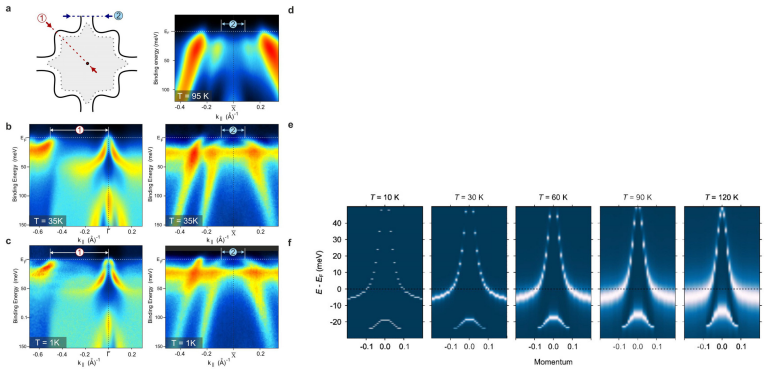

Fig. 14. $YbRh_2Si_2$: Temperature dependent Fermi surface evolution. Left panel: The T dependence was studied looking at the characteristic segments of the BZ which are schematically depicted in (a). (b), (c) ?diagonal? and (d)-(f) ?neck? direction. Right panel: 4f spectral functions corresponding to the crystal electrical field ground state calculated for temperatures T =10, 30, 60, 90, and 120 K around the ?neck? feature of the BZ. The necks of the BZ remain open until well above 120 K, in accordance with the experimental result. To better visualize the changes in the distribution of 4f spectral weight, the spectra were normalized to the maximum value at the temperature under consideration.

$$\mathbf{G_f}\left(\mathbf{k};\omega\right) = \mathbf{G_{f;loc}}\left(\mathbf{k};\omega\right) - \left(\mathbf{W}\left(\mathbf{k};\omega\right) - \mathbf{w}\left(\omega\right)\right) \tag{16}$$

where k and ω denote wave vector and frequency, $\mathbf{G}_{f;loc}(\omega)$ is the fully renormalized local f-Green's function and $\mathbf{W}$, w account for the hybridization with the conduction states. (For the notation see [42].)

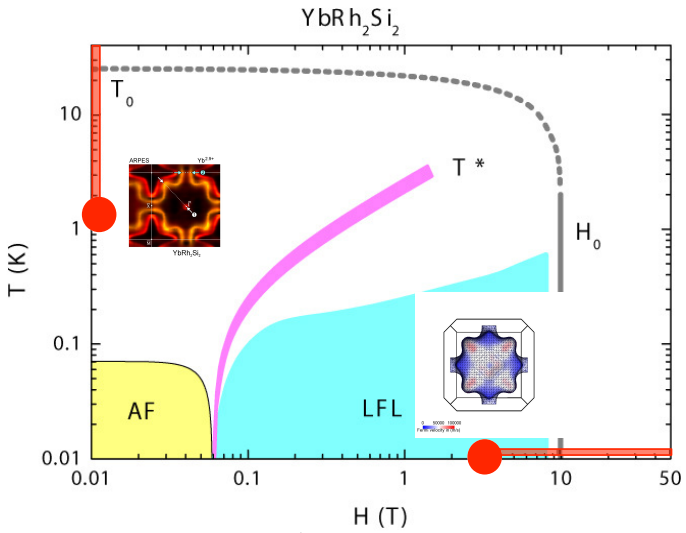

Fig. 15. $YbRh_2Si_2$: B-T phase diagram indicating the regions with "large" Fermi surface.

10. Summary and outlook

The central goal has been to characterize the states appearing in the phase diagram of $YbRh_2Si_2$ as displayed in Figure 15 and to eventually understand the physical origin of the various anomalies. The Renormalized Band results clearly show that $YbRh_2Si_2$ forms a strongly renormalized Fermi liquid in finite magnetic fields $B > 1T$, in agreement with the quadratic variation with temperature of the resistivity. The field-induced anomalies which are observed in transport properties result from Lifshitz-transitions of the "large" Fermi surface. High-resolution ARPEs data clearly show that the Fermi surface is "large" at $T > 1K$ in a vanishing magnetic field. The characteristics of the heavy quasiparticles are observed in the band dispersion up to rather temperatures. This behavior is consistent with theoretical calculations.

Considering the fact that we have a large Fermi surface on both the temperature and the magnetic-field axis leads us to question the Kondo break-down scenario for the T^*-line. This ansatz conjectures that the anomalies observed along the T^*-line are associated with the change in Fermi surface volume due to the break-down of the Kondo effect. On the other hand, our results seem to support the recent alternative "critical quasiparticle"

scenario which assumes the quasiparticles to be robust though modified by scattering from critical spin-fluctuations.

Acknowledgments

It is a great pleasure to thank E. Abrahams, S. Friedemann, P. Fulde, C. Geibel, A. C. Hewson, K. Kummer, H. Pfau, Q. Si, F. Steglich, P. Thalmeier, D. Vyalikh, S. Wirth, and P. Wölfle for many fruitful discussions. This research was supported in part by the National Science Foundation under Grant No. NSF PHY11-25915.

References

1. P. Fulde, *Correlated Electrons in Quantum Matter* (World Scientific Publishing Company, 2012).
2. S. Sachdev, *Quantum Phase Transitions*, 2nd edition edn. (Cambridge University Press, 2011).
3. G. R. Stewart, *Rev. Mod. Phys.* **73**, p. 797 (2001).
4. J. Flouquet, *Prog. Low Temp. Phys.* **15**, p. 139 (2005).
5. H. v. Löhneysen, A. Rosch, M. Vojta and P. Wölfle, *Rev. Mod. Phys.* **79**, 1015 (2007).
6. O. Stockert and F. Steglich, *Annu. Rev. Condens. Matter Phys.* **2**, 79 (2011).
7. A. C. Hewson, *The Kondo Problem to Heavy Fermions* (Cambridge University Press, 1993).
8. A. Sommerfeld and H. Bethe, Elektronentheorie der Metalle, in *Handbuch der Physik*, ed. A. Smekal (Springer, Berlin, Heidelberg, 1933) second edn.
9. L. D. Landau, *JETF* **30**, p. 1058 (1956).
10. L. D. Landau, The theory of a Fermi liquid, *JETP* **32**, p. 59 (1957).
11. L. D. Landau, *JETF* **35**, p. 97 (1958).
12. G. Baym and C. Pethick, Landau Fermi-liquid theory and low temperature properties of normal ^3He, in *The Physics of Liquid and Solid Helium, Part II*, eds. K. H. Bennemann and J. B. Ketterson (Wiley, New York, 1978) p. 1.
13. J. M. Luttinger and J. M. Ward, *Phys. Rev.* **118**, p. 1417 (1960).
14. J. M. Luttinger, *Phys. Rev.* **119**, p. 1153 (1960).
15. P. Hohenberg and W. Kohn, *Phys. Rev.* **136**, p. B864 (1964).
16. W. Kohn and L. Sham, *Phys. Rev.* **140**, p. A1133 (1965).
17. W. Kohn, *Rev. Mod. Phys.* **71**, 1253 (1999).

18. H. Eschrig, *The Fundamentals of Density Functional Theory* (Edition am Gutenbergplatz, 2003).
19. V. Sahni, *Quantal Density Functional Theory* (Springer, Berlin, 2004).
20. E. Engel and R. M. Dreizler, *Density Functional Theory: An Advanced Course (Theoretical and Mathematical Physics)* (Springer, 2011).
21. D. Sholl and J. A. Steckel, *Density Functional Theory* (John Wiley and Sons, 2014).
22. P. W. Anderson, *Basic Notions of Condensed Matter Physics*Frontiers in Physics Ser., no. 55 in Frontiers in Physics Ser. (Addison-Wesley, 1984).
23. J. C. Slater, **49**, 537, 931 (1936).
24. J. H. VanVleck, **25**, p. 220 (1953).
25. A. R. Mackintosh and O. K. Andersen, in *Electrons at the Fermi surface*, ed. M. Springford (Cambridge University Press, Cambridge, 1980)
26. P. Thalmeier and G. Zwicknagl, *Handbook on the Physics and Chemistry of Rare Earth* (Elsevier B. V., 2005), pp. 135–287.
27. P.Thalmeier, G. Zwicknagl, O. Stockert, G. Sparn and F. Steglich, *Frontiers in Superconducting Materials* (Springer, 2005), pp. 109–182.
28. F. Steglich, J. Arndt, O. Stockert, S. Friedemann, M. Brando, C. Klingner, C. Krellner, C. Geibel, S. Wirth, S. Kirchner and Q. Si, *J. Phys. Condens. Matter* **24**, p. 294201 (2012).
29. G. Zwicknagl, *Adv. Phys.* **41**, p. 203 (1992).
30. G. Zwicknagl, *Physica Scripta T* **49**, p. 34 (1993).
31. F. Reinert, D. Ehm, S. Schmidt, G. Nicolay, S. Hüfner, J. Kroha, O. Trovarelli and C. Geibel, *Phys. Rev. Lett.* **87**, p. 106401 (2001).
32. S. Ernst, S. Kirchner, C. Krellner, C. Geibel, G. Zwicknagl, F. Steglich and S.Wirth, *Nature* **to appear** (2011).
33. T. Kasuya, *Progress of Theoretical Physics Supplement* **108**, p. 1 (1992).
34. G. G. Lonzarich, *J. Magn. Magn. Mat.* **76 / 77**, p. 1 (1988).
35. H. Aoki, S. Uji, A. K. Albessard and Y. Onuki, *Phys. Rev. Lett.* **71**, p. 2110 (1993).
36. F. S. Tautz, S. R. Julian, G. J. McMullen and G. G. Lonzarich, *Physica B* **206-207**, p. 29 (1995).
37. J. D. Denlinger, G.-H. Gweon, J. W. Allen, C. G. Olson, Y. Daliachaouch, B.-W. Lee, M. B. Maple, Z. Fisk, P. C. Canfield and P. E. Armstrong, *Physica B* **281 & 282**, p. 716 (2000).
38. J. D. Denlinger, G.-H. Gweon, J. W. Allen, C. G. Olson, M. B. Maple, , J. L. Sarrao, P. E. Armstrong, Z. Fisk and H. Yamagami, *J. Electron*

Spectrosc. Relat. Phenom. **117 & 118**, p. 347 (2001).
39. C. Jayprakash, H.-R. Krishna-murthy and J. W. Wilkins, *Phys. Rev. Lett.* **47**, p. 737 (1981).
40. C. Jayprakash, H.-R. Krishna-murthy and J. W. Wilkins, *J. Appl. Phys.* **53**, p. 2142 (1982).
41. B. Jones and C. M. Varma, *J. Magn. Magn. Mater.* **63 & 64**, p. 251 (1987).
42. P. Fulde, J. Keller and G. Zwicknagl, Theory of heavy fermion systems, in *Solid State Physics*, eds. F. Seitz, D. Turnbull and H. Ehrenreich (Academic Press, New York, 1988) p. 1.
43. E. Runge and G. Zwicknagl, *Ann. Phys.* **5**, p. 333 (1996).
44. G. Zwicknagl, *J. Phys.: Condens. Matter* **22**, p. 115802 (2011).
45. P. Fulde, P. Thalmeier and G. Zwicknagl, *Solid State Physics* (Academic Press, 2006), ch. Strongly correlated electrons, p. 1.
46. P. Nozières, *J. Low Temo. Phys.* **17**, p. 31 (1974).
47. A. C. Hewson, A. Oguri and D. Meyer, *The European Physical Journal B - Condensed Matter and Complex Systems* **40**, 177 (2004).
48. A. C. Hewson, J. Bauer and W. Koller, *Phys. Rev. B* **73**, p. 045117 (2006).
49. J. Bauer and A. C. Hewson, *Phys. Rev. B* **76**, p. 035119 (2007).
50. R. Peters, T. Pruschke and F. B. Anders, *Phys. Rev. B* **74**, p. 245114 (2006).
51. A. C. Hewson, *J. Phys. Condens. Matter* **13**, p. 10011 (2001).
52. K. Edwards and A. C. Hewson, *J. Phys. Condens. Matter.* **23**, p. 045601 (2010).
53. K. Edwards, A. C. Hewson and V. Pandis, *Phys. Rev. B* **87**, p. 165128 (2013).
54. O. K. Andersen, *Phys. Rev. B* **12**, p. 3060 (1975).
55. H. Skriver, *The LMTO Method*, Springer Series in Solid State Sciences, Vol. 41 (Springer-Verlag, Berlin, 1984).
56. N. E. Christensen, *Int. Journ. Quantum Chem.* **XXV**, p. 233 (1984).
57. F. Steglich, U. Rauchschwalbe, U. Gottwick, H. M. Mayer, G. Sparn, N. Grewe and U. Poppe, *J. Appl. Phys.* **57**, p. 3054 (1985).
58. L. P. Regnault, W. A. C. Erkelens, J. Rossat-Mignot, P. Lejay and J. Flouquet, *Phys. Rev. B* **38**, p. 4481 (1988).
59. G. Zwicknagl, E. Runge and N. E. Christensen, **163**, p. 97 (1990).
60. A. K. Albessard, T. Ebihara, I. Umehara, K. Satoh, Y. Onuki, H. Aoki, S. Uji and T. Shimizu, *Physica B* **186-188**, p. 147 (1993).
61. G. Bruls, D. Weber, B. Wolf, P. Thalmeier, B. L"uthi, A. de Visser

and A. Menovsky, *Phys. Rev. Lett.* **65**, p. 2294 (1990).
62. F. W. et al., (2004).
63. E. A. Goremychkin and R. Osborn, *Phys. Rev. B* **47**, p. 14280 (1993).
64. G. Zwicknagl and U. Pulst, **186**, p. 895 (1993).
65. U. Pulst, Dissertation TH Darmstadt1993.
66. P. Gegenwart, C. Langhammer, C. Geibel, R. Helfrich, M. Lang, G. Sparn, F. Steglich, R. Horn, L. Donnevert, A. Link and W. Assmus, *Phys. Rev. Lett.* **81**, p. 1501 (1998).
67. F. Steglich, N. Sato, T. Tayama, T. Lühmann, C. Langhammer, P. Gegenwart, P. Hinze, C. Geibel, M. Lang, G. Sparn and W. Assmus, *Physica C* **341-348**, p. 691 (2000).
68. O. Stockert, E. Faulhaber, G. Zwicknagl, N. Stüßer, H. S. Jeevan, M. Deppe, R. Borth, R. Küchler, M. Loewenhaupt, C. Geibel and F. Steglich, *Phys. Rev. Lett* **92**, p. 136401 (2004).
69. P. Gegenwart, Y. Tokiwa, T. Westerkamp, F. Weickert, J. Custers, J. Ferstl, C. Krellner, C. Geibel, P. Kerschl, K.-H. Müller and F. Steglich, *New Journal of Physics* **8**, p. 171 (2006).
70. P. Gegenwart, Q. Si and F. Steglich, *Nature Phys.* **4**, p. 186 (2008).
71. P. Gegenwart, J. Custers, C. Geibel, K. Neumeier, T. Tayama, K. Tenya, O. Trovarelli and F. Steglich, *Phys. Rev. Lett.* **89**, p. 056402 (2002).
72. S. Friedemann, S. Wirth, N. Oeschler, C. Krellner, C. Geibel, F. Steglich, S. MaQuilon, Z. Fisk, S. Paschen and G. Zwicknagl, *Phys. Rev. B* **82**, p. 035103 (2010).
73. S. F. andSwee K Goh, P. M. C. Rourke, P. Reiss, M. L. Sutherland, F. M. Grosche, G. Zwicknagl and Z. Fisk,*New J. Phys.* **15**, p. 093014 (2013).
74. O. Stockert, M. Koza, J. Ferstl, A. Murani, C. Geibel and F. Steglich, *Physica B: Condensed Matter* **378-380**, 157 (2006).
75. A. Hiess, O. Stockert, M. Koza, Z. Hossain and C. Geibel *Physica B: Condensed Matter* **378-380**, 748 (2006).
76. G. Zwicknagl, Quasiparticles, magnetization dynamics, and thermopower of Yb-based heavy-fermion compounds, in *Properties and Applications of Thermoelectric Materials*, eds. V. Zlatic and A. C. Hewson, NATO Science for Peace and Security Series B: Physics and Biophysics, Vol. 133 (Springer, Berlin, 2009).
77. G. Zwicknagl, *J. Phys. Soc. Jpn.* **80**, p. SA010 (2011).
78. G. Knebel, R. Boursier, E. Hassinger, G. Lapertot, P. G. Niklowitz, A. Pourret, B. Salce, J. P. Sanchez, I. Sheikin, P. Bonville, H. Harima

and J. Flouquet, *J. Phys. Soc. Jpn.* , p. 114709 (2006).
79. T. Jeong, *Journal of Physics: Condensed Matter* **18**, 10529 (2006).
80. P. M. C. Rourke, A. McCollam, G. Lapertot, G. Knebel, J. Flouquet and S. R. Julian, *Phys. Rev. Lett.* **101**, p. 237205 (2008).
81. P. M. C. Rourke, A. McCollam, G. Lapertot, G. Knebel, J. Flouquet and S. R. Julian, *Journal of Physics: Conference Series* **150**, p. 042165 (2009).
82. A. B. Sutton, P. M. C. Rourke, V. Taufour, A. McCollam, G. Lapertot, G.and Knebel, J. Flouquet and S. R. Julian, *physica status solidi (b)* **247**, 549 (2010).
83. G. A. Wigger, F. Baumberger, Z.-X. Shen, Z. P. Yin, W. E. Pickett, S. Maquilon and Z. Fisk, *Phys. Rev. B* **76**, p. 035106 (2007).
84. Y. Tokiwa, P. Gegenwart, T. Radu, J. Ferstl, G. Sparn, C. Geibel and F. Steglich, *Phys. Rev. Lett.* **94**, 226402 (2005).
85. H. Pfau, R. Daou, S. Lausberg, H. Naren, M. Brando, S. Friedemann, S. Wirth, T. Westerkamp, U. Stockert, P. Gegenwart, C. Krellner, C. Geibel, G. Zwicknagl and F. Steglich, *Phys. Rev. Lett.* **110**, p. 256403 (2013).
86. A. Pourret, G. Knebel, T. D. Matsuda, G. Lapertot and J. Flouquet, *J. Phys. Soc. Jpn.* **82**, p. 053704 (2013).
87. T. Westerkamp, PhD thesis, Technische Universität Dresden2009.
88. K. Kummer, S. Patil, A. Chikina, M. Güttler, M. Höppner, A. Generalov, S. Danzenbächer, S. Seiro, A. Hannaske, C. Krellner, Y. Kucherenko, M. Shi, M. Radovic, E. Rienks, G. Zwicknagl, K. Matho, J. Allen, C. L. andC. Geibel and D. V. Vyalikh, *Phys. Rev. X* **5** (2015).